Journal of Molecular Graphics and Modelling 27 (2009) 853–859

Contents lists available at ScienceDirect

Journal of Molecular Graphics and Modelling

journal homepage: www.elsevier.com/locate/JMGM

Computed NMR shielding increments over unsaturated five-membered ring heterocyclic compounds as a measure of aromaticity

Ned H. Martin *, Jimmy E. Rowe, Eddie LaReece Pittman

Department of Chemistry and Biochemistry, University of North Carolina Wilmington, 601 South College Road, Wilmington, NC 28403-5932, USA

ARTICLE INFO

Article history:
Received 10 December 2008
Received in revised form 31 December 2008
Accepted 13 January 2009
Available online 22 January 2009

Keywords:
NMR shielding
GIAO
Aromaticity
Conjugated five-membered heterocyclic rings

ABSTRACT

The GIAO-HF method within Gaussian 03 was used to calculate the isotropic shielding value of the proximal hydrogen of a diatomic hydrogen probe at various distances (2.5 Å, 3.0 Å and 4.0 Å) above the plane of 15 conjugated five-membered ring heterocyclic compounds: pyrrole, furan, thiophene, and phosphole and their 2- and 3-nitrogen analogs. Subtraction of the isotropic shielding value of diatomic hydrogen by itself from each of these isotropic shielding values gave the shielding increment ($\Delta\sigma$) for each probe position. Plotting $\Delta\sigma$ against Cartesian coordinates of the probe position allowed determination of the computed through-space shielding increment surfaces for these compounds. Substantial shielding was observed above the center of each ring, as expected for aromatic compounds. The magnitude of the shielding increment at 2.5 Å above the ring center ($\Delta\sigma_{2.5}$) correlated reasonably well with other established methods of assessing aromaticity, including geometric (HOMA, harmonic oscillator model of aromaticity), energetic (ASE, aromatic stabilization energy), and magnetic (NICS, nucleus-independent chemical shift) criteria.

© 2009 Elsevier Inc. All rights reserved.

1. Introduction

Numerous methods have been developed for the measurement of the extent of aromaticity since Kekulé first introduced the concept 144 years ago [1], but no single measure has gained universal acceptance. Part of the problem is that aromaticity is a multidimensional property, composed of geometrical, energetic and magnetic components, whereas most measures focus on only one aspect [2]. For example, the harmonic oscillator model of aromaticity, HOMA [3–6] relies on the degree of bond length similarity. Others rely on energetics, such as aromatic stabilization energy, ASE [7–11]. A third category of methods depends on the magnetic properties; these include exaltation of magnetic susceptibility, Λ [12–14], anisotropy of the magnetic susceptibility [15], nuclear magnetic resonance shifts [16–18], and nucleus-independent chemical shifts, NICS, a measure of the diatropic (for aromatic compounds) or paratropic (for antiaromatic compounds) ring current [19,20]. NICS or one of its variations, such as aromatic ring current shieldings (ARCS) computed from NICS measurements perpendicular to the plane of aromatic rings [21], Kleinpeter's [22,23] graphical maps of NICS, named isochemical shielding surfaces (ICSS), or Stanger's partitioned NICS [24] are perhaps the more common methods in use today to measure or predict aromaticity. Cyrański et al. [25,26] showed that for a series of 75 five-membered ring π-electron systems and 30 ring-substituted compounds (including aromatic, nonaromatic and antiaromatic systems), loose correlations exist among the four most widely used measures of aromaticity: ASE, Λ, HOMA and NICS. NICS measurements have become the most widely used measure of aromaticity, but they have limitations in terms of predicting aromaticity vs. antiaromaticity. For instance, the NICS value of the antiaromatic cyclopropenyl anion is negative, indicative of an aromatic structure. Correct assignments of aromaticity and antiaromaticity are obtained if a probe molecule, such as diatomic hydrogen, is used to determine the through-space shielding effect [27]. In contrast, the NICS method involves computing the magnetic shielding at a point in space.

We have reported the results of GIAO-HF calculations to calculate through-space NMR shielding effects on a probe molecule and to map the resulting through-space NMR shielding increments in aromatic ring π-stacked complexes [28]. More recently the computed shielding effects of linear polycyclic aromatic hydrocarbons (PAHs) [29] and the relationship between the computed shielding effects and the extent of aromaticity have been reported.

2. Computational methods

Structures of the conjugated five-membered ring heterocyclic compounds in this study are shown in Fig. 1. They consist of pyrrole

* Corresponding author. Tel.: +1 9109623453; fax: +1 9109623013.
E-mail address: martinn@uncw.edu (N.H. Martin).

1093-3263/$ – see front matter © 2009 Elsevier Inc. All rights reserved.
doi:10.1016/j.jmgm.2009.01.002

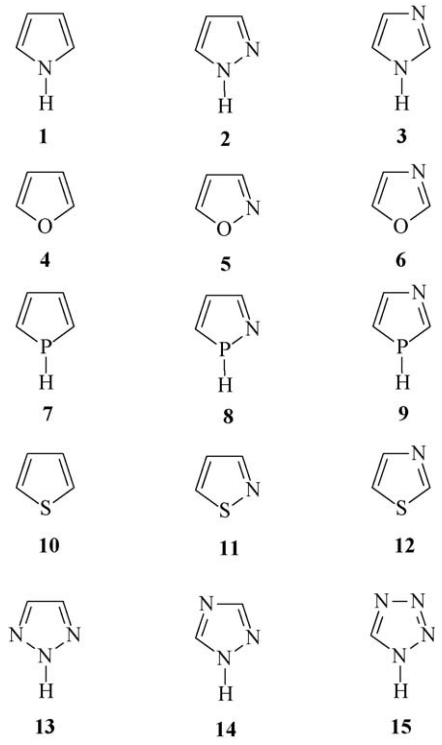

Fig. 1. Structures of the five-membered ring heterocyclic compounds in the study.

(**1**), furan (**4**), phosphine (**7**) and thiophene (**10**) and their α-aza (**2**, **5**, **8**, and **11**) and β-aza derivatives (**3**, **6**, **9**, and **12**), plus several multi-aza derivatives of pyrrole (**13**, **14** and **15**). A model of each of these was built in Titan [30], and equilibrium geometries were obtained at the Hartree-Fock level of theory using the 6-31G(d,p) basis set [31]. These structures are all planar, which allowed the Cartesian coordinate molecule description to be oriented with the carbon atoms in the XY plane having the center of the molecule at the origin of Cartesian space and one heteroatom along the negative Y axis. A diatomic hydrogen (H_2) probe [32], previously geometry optimized at HF/6-31G(d,p), was placed along the Z axis with the proximal hydrogen at a distance of 2.5 Å from the plane of each molecule. A series of single point NMR calculations[1] was performed in Gaussian 03 [33] on these supramolecules using the same method and basis set, moving the H_2 in 1.0 Å increments in both the X and Y directions in separate calculations. Calculations were also performed with the diatomic hydrogen probe above the geometric midpoint of each ring. The process was repeated with the H_2 probe at proximate hydrogen distances of 3.0 Å and 4.0 Å from the plane of the molecule being studied. These calculations covered a grid that extended beyond the positions of the carbon atoms in the X and Y directions. The symmetry of some of the structures allowed only one-half of the grid to be calculated and the data to be replicated by a reflection across the Y axis. The shielding increment ($\Delta\sigma$) at a given point in Cartesian space was determined by taking the difference between the calculated isotropic shielding value of one of the hydrogens in the H_2 probe alone (26.77 ppm) and that of the proximal hydrogen of the H_2 probe at that point relative to the heterocyclic structures. Computed isotropic shift values greater than that of isolated H_2 result in positive (shielding) $\Delta\sigma$ values; those with smaller values yield negative (deshielding) $\Delta\sigma$ values. The shielding increments ($\Delta\sigma$) are therefore equal in magnitude but opposite in sign to differences in ^{1}H-NMR chemical shifts ($\Delta\delta$). Three-dimensional NMR shielding increment surfaces ($\Delta\sigma$ vs. *X* and *Y* at a fixed value of *Z*) were prepared using TableCurve 3D [35] to represent graphically the locations and magnitudes of shielding over the molecules in the study.

Linear correlations were determined for shielding increments computed 2.5 Å over the ring centers ($\Delta\sigma_{2.5}$) against various other measures of aromaticity for these compounds collected by Cyrański [25]. These include HOMA, ASE, and NICS(1) values.

3. Results and discussion

Shielding increment surfaces 2.5 Å, 3.0 Å and 4.0 Å above the plane of pyrrole are shown in Fig. 2. By far the greatest shielding (and deshielding) is found close to plane of the aromatic compound. The shielding increment surfaces for 3.0 Å and 4.0 Å for each of the other compounds in this study are similarly less featured than those at 2.5 Å and have smaller shielding and deshielding values; for that reason, only shielding increment surfaces at 2.5 Å will be shown henceforth. Shielding increment surfaces at 2.5 Å above the plane of pyrrole **1** and its α-aza and β-aza derivatives (1H-pyrazole **2** and 1H-imidazole **3**) are shown in Fig. 3. Each of the shielding increment surfaces shows a dominant mound of shielding near the center of the ring and a region of slight deshielding beyond the vicinity of the additional heteroatom. The maximum shielding value ($\Delta\sigma_{2.5}$, taken at the center of the ring) and the minimum shielding value ($\Delta\sigma_{min}$, typically found beyond the heteroatom) for each structure in the study are collected in Table 1, along with several other published measures of the extent of aromaticity: ASE, HOMA, and NICS(1) taken from Cyrański [25]. Published data were not available (na) for some of the structures in this study.

The maximum shielding observed over the surfaces of the oxygen-containing heterocyclic structures furan **4**, isoxazole **5** and oxazole **6** (Fig. 4) is somewhat less than that observed over pyrrole and its aza analogs. As with the aza derivatives of pyrrole, deshielding is observed in the region beyond the nitrogen. The magnitude of deshielding is also slightly less than that found in pyrrole and its aza analogs.

Phosphole **7** and its aza analogs isophosphazole **8** and phosphazole **9** show very different shielding increment surfaces from pyrrole, furan and their aza analogs. Structural differences offer an explanation. Phosphole and its analogs have a pyramidal phosphorus with a lone pair of electrons projecting from the plane on one side of the ring and a P–H bond projecting from the plane on the other side. Separate calculations were performed on phosphole and its analogs with the diatomic hydrogen probe on both sides of the ring. Interestingly, the qualitative results are very similar. Regardless of which side the probe was placed, the maximum shielding increment over the ring center is much less than is observed over pyrrole, furan, and their aza analogs. In addition, a region of substantial deshielding is observed beyond the phosphorus. The shielding increment surfaces computed with the diatomic hydrogen probe molecule on the lone pair side (opposite the P–H bond) are presented in Fig. 5; those with the probe on the P–H bond side are shown in Fig. 6. The major differences are quantitative. The maximum shielding increment, which is less that that observed in the pyrrole and furan series, is greater over the ring center on the lone pair side (Table 1). In phosphole **7** and phosphazole **9**, the maximum deshielding is substantial (−1.67 to −1.93 ppm), and is also greater on the lone pair side by nearly 0.5 ppm. In isophosphazole **8** the maximum deshielding increments (−1.35 to −1.41 ppm) are very similar on both sides. As observed previously in the pyrrole and furan series, slight deshielding occurs beyond the nitrogen heteroatom in all aza analogs.

[1] Previous calculations [28] have shown that basis set superposition error, as measured by the counterpoise method of Boys and Bernardi [34], has a negligible effect on shielding values. BSSE is typically no greater than 0.05 ppm. Furthermore, the difference between the shielding values obtained using single point calculations and constrained geometry-optimized calculations is also negligible [32].

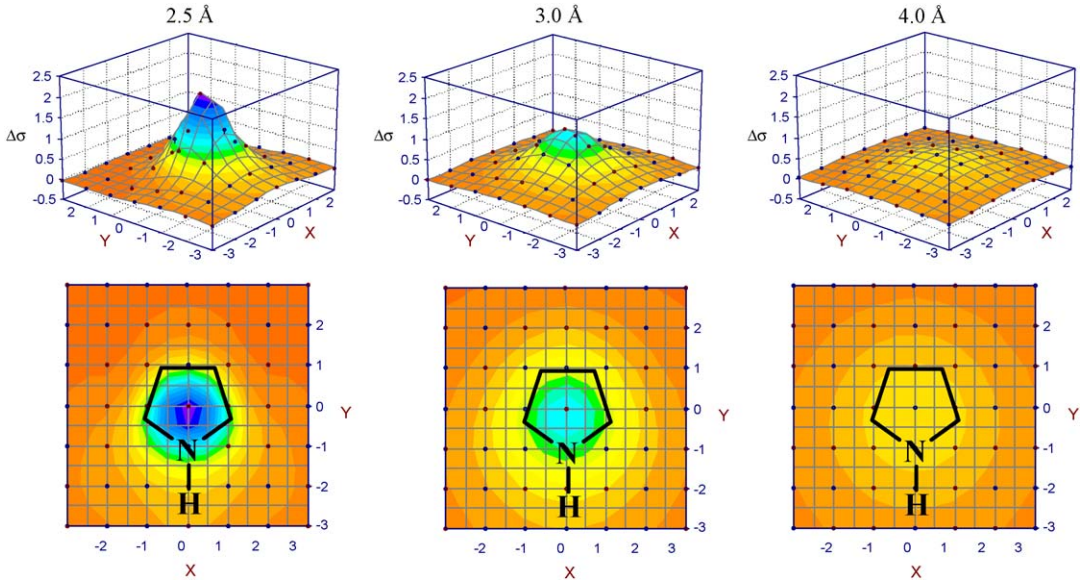

Fig. 2. Calculated shielding increment surfaces (in ppm) of pyrrole at 2.5 Å, 3.0 Å, and 4.0 Å.

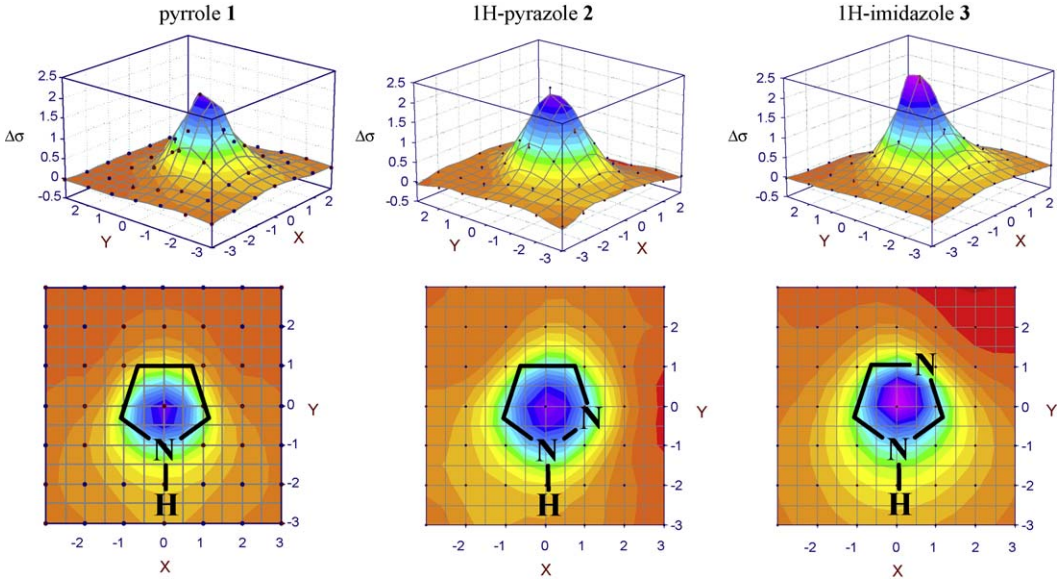

Fig. 3. Calculated shielding increment surfaces (in ppm) of pyrrole, 1H-pyrazole, and 1H-imidazole at 2.5 Å.

Table 1
Maximum and minimum shielding increments ($\Delta\sigma_{2.5}$ and $\Delta\sigma_{min}$, in ppm) calculated 2.5 Å above the plane of the indicated compound, along with aromatic stabilization energies (ASE, in kcal/mol), harmonic oscillator model of aromaticity (HOMA, unitless) values, and nucleus-independent chemical shift (NICS(1), in ppm) values tabulated by Cyrański [25].

Compound	$\Delta\sigma_{2.5}$ (ppm)	$\Delta\sigma_{min}$ (ppm)	ASE (kcal/mol)	HOMA	NICS(1) (ppm)
Pyrrole **1**	2.04	−0.06	20.57	0.876	−10.60
1H-Pyrazole **2**	2.29	−0.14	23.70	0.926	−11.93
1H-Imidazole **3**	2.29	−0.26	18.78	0.908	−10.83
Furan **4**	1.79	−0.03	14.77	0.298	−9.36
Isoxazole **5**	1.97	−0.16	17.29	0.527	−10.58
Oxazole **6**	2.15	−0.15	12.37	0.332	−9.45
Phosphole **7** (lp side)	1.53	−1.93	na	na	na
Phosphole **7** (P–H side)	1.19	−1.47	na	na	na
Phosphole **7** (mean)	1.36	na	3.20	0.236	−5.97
Isophosphazole **8** (lp side)	1.77	−1.35	na	na	na
Isophosphazole **8** (P–H side) side)	1.56	−1.41	na	na	na
Isophosphazole **8** (mean)	1.66	na	3.34	na	−6.84
Phosphazole **9** (lp side)	1.82	−1.67	na	na	na
Phosphazole **9** (lp side)	1.48	−1.23	na	na	na
Phosphazole **9** (mean)	1.65	na	3.01	0.276	−6.25

Table 1 (*Continued*)

Compound	$\Delta\sigma_{2.5}$ (ppm)	$\Delta\sigma_{min}$ (ppm)	ASE (kcal/mol)	HOMA	NICS(1) (ppm)
Thiophene **10**	2.39	−0.59	18.57	0.891	−10.79
Isothiazole **11**	2.63	−0.43	20.18	na	−11.66
Thiazole **12**	2.54	−0.44	17.43	0.905	−11.37
1,2,3-Triazole **13**	2.72	−0.05	26.66	0.960	−13.61
1,2,4-Triazole **14**	2.51	−0.20	21.33	0.940	−11.84
1H-Tetrazole **15**	2.92	−0.22	18.26	0.897	−14.12

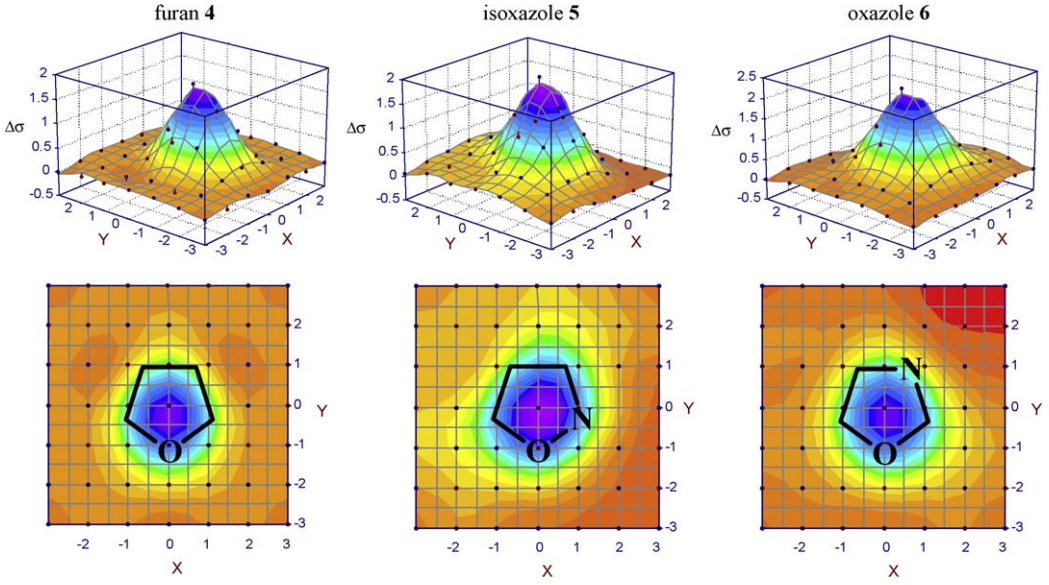

Fig. 4. Calculated shielding increment surfaces (in ppm) of furan, isoxazole, and oxazole at 2.5 Å.

Thiophene and its aza analogs display substantial shielding over their ring centers and moderate deshielding beyond the sulfur (and nitrogen heteratom in the aza analogs; Fig. 7). The maximum shielding increment (2.39–2.63 ppm) over thiophene and its aza analogs is greater than over pyrrole, furan, or phosphole and their aza analog (Table 1), but the greatest deshielding (−0.43 to −0.59 ppm) is much less deshielding than that observed in the phosphole series.

The substantial deshielding seen near sulfur and phosphorus (Figs. 5–7) is expected owing to their larger van der Waals radii (1.82 Å and 1.85 Å, respectively) as compared to nitrogen and oxygen (1.53 Å and 1.50 Å, respectively) [36]. An explanation of the greater deshielding in phosphine and its aza analogs (compared to thiophene and its aza analogs) is related to the fact that thiophene is more aromatic than phosphine. One of the lone pairs of electrons of thiophene is much more involved in delocalization with the

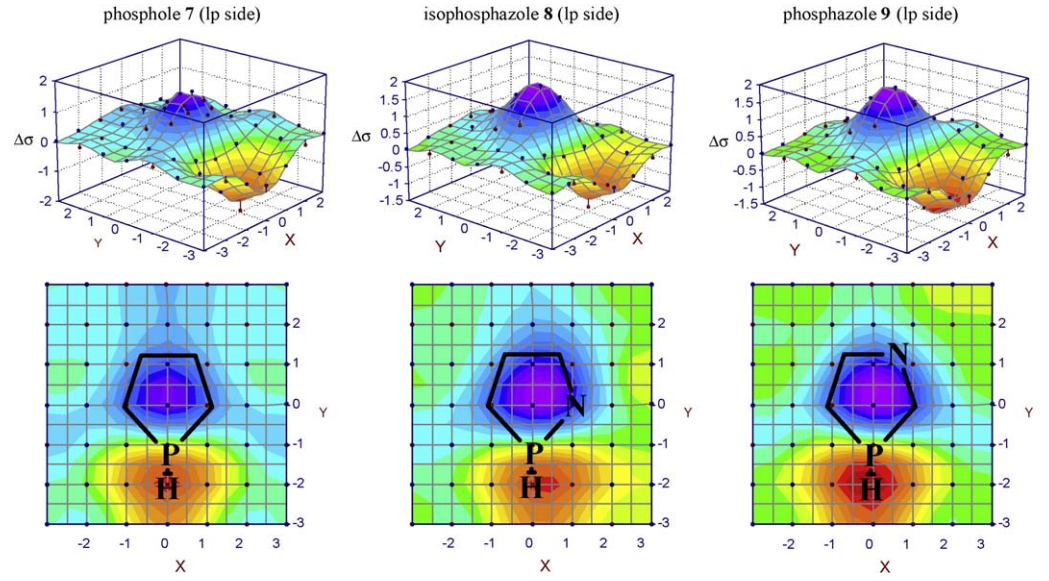

Fig. 5. Calculated shielding increment surfaces (in ppm) of phosphole (lp side), isophosphole (lp side), and phosphazole (lp side) at 2.5 Å.

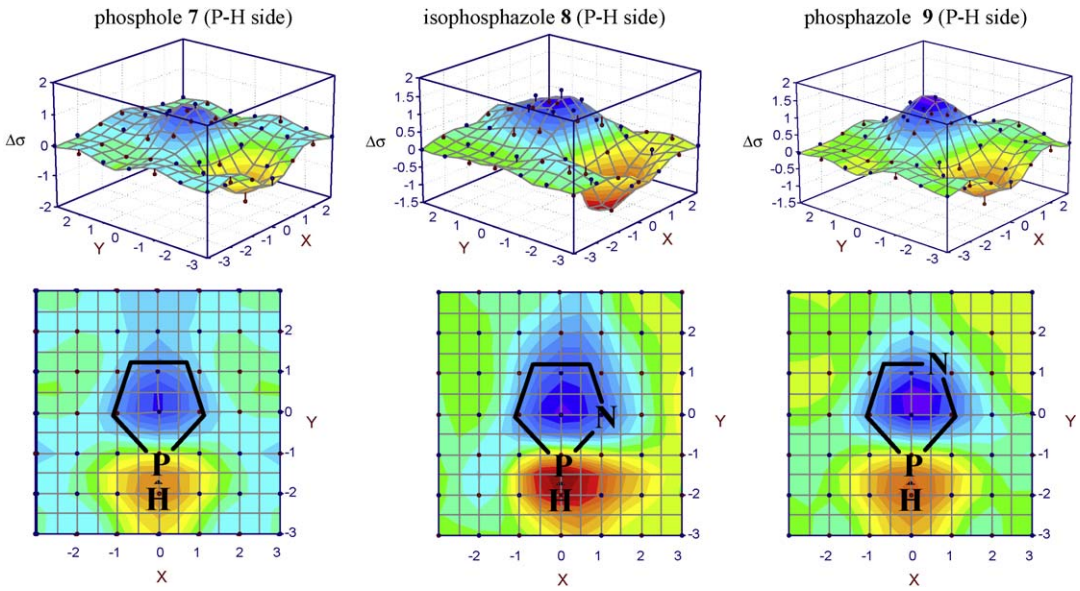

Fig. 6. Calculated shielding increment surfaces (in ppm) of phosphole (P–H side), isophosphole (P–H side), and phosphazole (P–H side) at 2.5 Å.

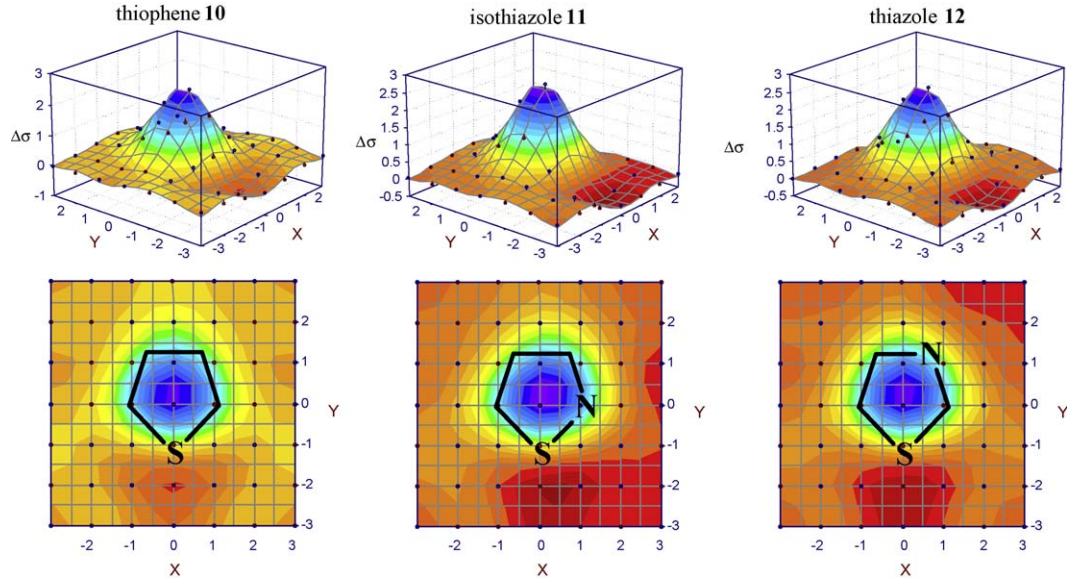

Fig. 7. Calculated shielding increment surfaces (in ppm) of thiophene, isothiazole, and thiazole at 2.5 Å.

other π-electrons, leading to a greater ring current and therefore greater shielding over the ring center, as observed ($\Delta\sigma_{2.5}$ = 2.4 ppm over thiophene vs. 1.4 ppm over phosphole). The other lone pair of electrons on sulfur can be thought to occupy an sp^2 hybrid orbital in the plane of the molecule. In phosphole, on the other hand, the lone pair of electrons is more localized on the pyramidal phosphorus, leading to less aromaticity, less ring current, and therefore less shielding over the ring center. Furthermore, localized electrons give rise to greater van der Waals deshielding. The P–H bond projecting from the molecular plane also causes substantial van der Waals deshielding.

In Fig. 8 are shown the shielding increment surfaces of analogs of pyrrole having three and four nitrogens (1,2,3-triazole **13**, 1,2,4-triazole **14**, and 1H-tetrazole **15**). The shapes of the surfaces are reminiscent of the shielding increment surfaces of other pyrrole derivatives, showing mounds of substantial shielding over the ring center and regions of deshielding beyond the nitrogen heteratoms. The maximum shielding increments over the nitrogen analogs of pyrrole having three or four nitrogen atoms in the ring are the highest of any in the study (2.5–2.9 ppm). Each additional nitrogen adds 0.2–0.3 ppm to the maximum shielding increment observed over the ring center. Because nitrogen is the only additional heteroatom incorporated in any of the ring systems in this study, no conclusions can be drawn regarding the origin of this effect.

Linear correlations were determined between the $\Delta\sigma_{2.5}$ values computed in this study and other published measures of aromaticity collected by Cyrański [25]. The NICS(1) values reported for phosphole and its aza analogs are the mean of the NICS(1) computed on the P–H side and that computed on the lone pair side (opposite the P–H bond) [37]. For that reason, mean values of $\Delta\sigma_{2.5}$ for phosphole and its aza analogs were also used in the correlations. The coefficients of determination (r^2 values) for each correlation are shown in Table 2. From the data it is clear that no single measure of aromaticity correlates highly with any other measure. This has been well documented, and supports the multidimensional nature of aromaticity. However, it is also evident

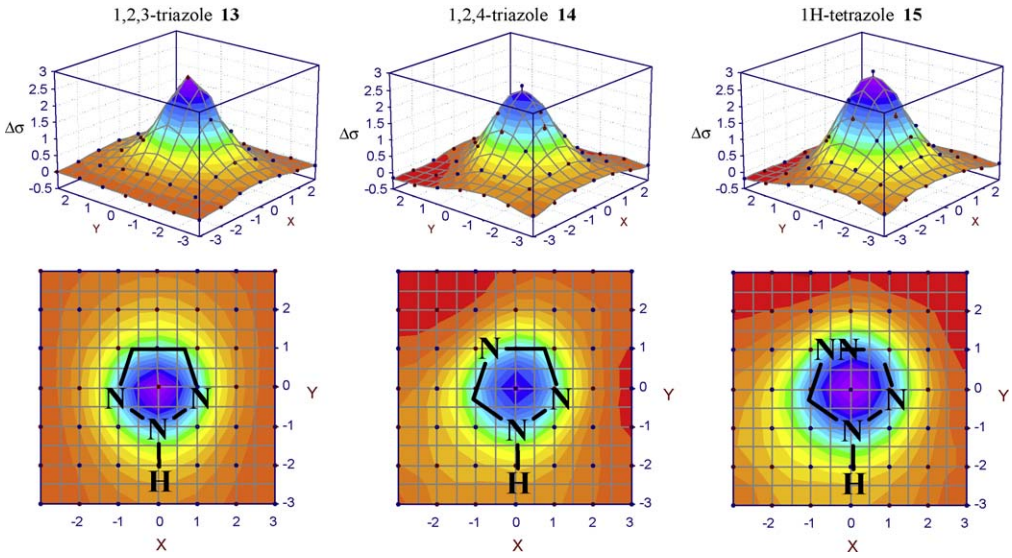

Fig. 8. Calculated shielding increment surfaces (in ppm) of 1,2,3-triazole, 1,2,4-triazole, and 1H-tetrazole, at 2.5 Å.

Table 2
Coefficients of determination (r^2) for linear correlation of this study's $\Delta\sigma_{2.5}$ values (ppm) vs. published measures of aromaticity [25]. For phosphole and its aza analogs, mean $\Delta\sigma_{2.5}$ values of those calculated both on the side of the lone pair of electrons and on the P–H bond side were used in the correlations. The mean r^2 values of each measure's correlation with the other three are shown in bold.

	r^2 of linear correlation			
	$\Delta\sigma_{2.5}$	ASE	HOMA	NICS(1)
$\Delta\sigma_{2.5}$	–	0.64	0.69	0.88
ASE	0.64	–	0.73	0.85
HOMA	0.69	0.73	–	0.70
NICS(1)	0.88	0.85	0.70	–
Mean r^2	**0.74**	**0.74**	**0.71**	**0.81**

from the data in Table 2 that $\Delta\sigma_{2.5}$ values correlate with the other measures the same as ASE, slightly better than HOMA, but not quite as well as NICS(1) values do. The advantage of shielding increment values (and the 3D shielding surface maps) over NICS values is that shielding increments have been shown to be reliable predictors of chemical shifts of protons as a function of position over the molecule in question, whereas NICS do not reliably predict chemical shift effects [32]. This is due in part to the fact that $\Delta\sigma$ values, unlike NICS measurements, include orbital interactions and polarizability, both important aspects of the net magnetic shielding experienced by protons near π-electron systems [38].

4. Conclusions

NMR shielding calculations have been performed with the proximal hydrogen of a diatomic hydrogen probe juxtaposed at various positions over a series of 15 conjugated five-membered ring heterocyclic compounds. Subtraction of the shielding value of diatomic hydrogen by itself gives the shielding increment ($\Delta\sigma$). Plots of the shielding increment vs. Cartesian coordinates provide shielding increment surfaces for each of the heterocycles. Mounds of shielding are evident near the center of each ring, with slight deshielding in the region beyond the heteroatom(s). With phosphole, thiophene and their aza analogs, substantial deshielding was observed beyond their sulfur or phosphorus heteratom, attributed to van der Waals deshielding. Linear correlations between the maximum computed shielding 2.5 Å above each ring ($\Delta\sigma_{2.5}$) and various published measures of aromaticity, including those related to energy (ASE), geometry (HOMA) and magnetic properties (NICS) show that $\Delta\sigma_{2.5}$ correlates with the other measures slightly better than HOMA, the same as ASE, and almost as well as NICS(1).

Acknowledgments

The authors gratefully acknowledge East Carolina University for use of their computational facilities and the donors of the Petroleum Research Fund, administered by the American Chemical Society, for support of this work.

References

[1] A. Kekulé, Sur la constitution des substances aromatiques, Bull. Soc. Chim. Fr. (Paris) 3 (2) (1865) 98–110.
[2] P.V.R. Schleyer, Introduction: aromaticity, Chem. Rev. 101 (5) (2001) 1115–1118.
[3] T.M. Krygowski, Crystallographic studies of inter- and intramolecular interactions reflected in aromatic character of π-electron systems, J. Chem. Inf. Comput. Sci. 33 (1) (1993) 70–78.
[4] T.M. Krygowski, M.K. Cyrański, Separation of the energetic and geometric contributions to the aromaticity of π-electron carbocyclics, Tetrahedron 52 (5) (1996) 1713–1722.
[5] T.M. Krygowski, M.K. Cyrański, Aromatic character of carbocyclic π-electron systems deduced from molecular geometry, in: M. Hargittai, I. Hargittai (Eds.), Advances in Molecular Structure Research, vol. 3, JAI Press, London, 1997 pp. 227–268.
[6] T.M. Krygowski, M.K. Cyrański, Structural aspects of aromaticity, Chem. Rev. 101 (5) (2001) 1385–1419.
[7] W.J. Hehre, R.T. McIver, J.A. Pople, P.V.R. Schleyer, Alkyl substituent effects on the stability of protonated benzene, J. Am. Chem. Soc. 96 (1974) 7162–7163.
[8] P. George, M. Trachtman, A.M. Brett, C.W. Bock, Comparison of various isodesmic and homodesmotic reaction heats with values derived from published ab initio molecular orbital calculations, J. Chem. Soc., Perkin Trans. 2 (1977) 1036–1047.
[9] C.H. Suresh, N. Koga, Accurate calculation of aromaticity of benzene and anti-aromaticity of cyclobutadiene: new homodesmotic reactions, J. Org. Chem. 67 (2002) 1965–1968.
[10] L.J. Schaad, B.A. Hess Jr., Dewar resonance energy, Chem. Rev. 101 (5) (2001) 1465–1476.
[11] J.F. Liebman, S.W. Slayden, The energetics of aromatic hydrocarbons: an experimental thermochemical perspective, Chem. Rev. 101 (5) (2001) 1541–1566.
[12] H.J. Dauben, J.D. Wilson, J.L. Laity, Diamagnetic susceptibility exaltation as a criterion of aromaticity, J. Am. Chem. Soc. 91 (8) (1969) 1991–1998.
[13] J. Hoarau, Magnetic properties of conjugated molecules, J. Ann. Chim. 13 (1) (1956) 544–587.
[14] A. Pacault, Magnetochemical studies A, Ann. Chim. 12 (1) (1946) 527–587.
[15] W.H. Flygare, Magnetic interactions in molecules and an analysis of molecular electronic charge distribution from magnetic parameters, Chem. Rev. 74 (1974) 653–687.
[16] C.W. Haigh, R.B. Mallion, Ring current theories in nuclear magnetic resonance, in: J.W. Emsley, J. Feeny, L.H. Sutcliffe (Eds.), Progress in Nuclear Magnetic Resonance Spectroscopy, vol. 13, Pergamon Press, Oxford, UK, 1979–1980.
[17] J.A.N.F. Gomes, R.B. Mallion, The concept of ring currents, in: D.H. Rouvray (Ed.), Concepts in Chemistry: A Contemporary Challenge, Research Studies Press, Taunton, Somerset, UK, 1997, pp. 205–253.

[18] P. Lazzeretti, Ring currents, in: J.W. Emsley, J. Feeny, L.H. Sutcliffe (Eds.), Progress in Nuclear Magnetic Resonance Spectroscopy, vol. 36, Elsevier, Amsterdam, The Netherlands, 2000, pp. 1–88.
[19] P.V.R. Schleyer, C. Maerker, A. Dransfield, H. Jiao, N.J.R. van Eikema Hommes, Nucleus-independent chemical shifts: a simple and efficient aromaticity probe, J. Am. Chem. Soc. 118 (1996) 6317–6318.
[20] Z. Chen, C.S. Wannere, C. Corminboeuf, R. Puchta, P.V.R. Schleyer, Nucleus-independent chemical shifts (NICS) as an aromaticity criterion, Chem. Rev. 105 (10) (2001) 3842–3888.
[21] J. Jusélius, D. Sundholm, Ab initio determination of the induced ring current in aromatic molecules, Phys. Chem. Chem. Phys. 1 (1999) 3429–3435.
[22] S. Klod, E. Kleinpeter, *Ab initio* calculation of the anisotropy effect of multiple bonds and the ring current effect of arenes-application in conformational and configurational analysis, J. Chem. Soc. Perkin Trans. 2 (2001) 1893–1898.
[23] E. Kleinpeter, S. Klod, *Ab initio* calculation of the anisotropic/ring current effects of amino acid residues to locate the position of substrates in the binding site of enzymes, J. Mol. Struct. 704 (2004) 79–82.
[24] A. Stanger, Nucleus-independent chemical shifts (NICS): distance dependence and revised criteria for aromaticity and antiaromaticity, J. Org. Chem. 71 (3) (2006) 883–893.
[25] M.K. Cyrański, T.M. Krygowski, A.R. Katritsky, P.V.R. Schleyer, To what extent can aromaticity be defined uniquely? J. Org. Chem. 67 (4) (2002) 1333–1338.
[26] M.K. Cyrański, Energetic aspects of cyclic pi-electron delocalization: evaluation of the methods of estimating aromatic stabilization energies, Chem. Rev. 105 (10) (2005) 3773–3811 (and references cited therein).
[27] N.H. Martin, D.M. Loveless, K.L. Main, D.C. Wade, Computation of through-space NMR shielding effects by small-ring aromatic and antiaromatic hydrocarbons, J. Mol. Graphics Modell. 25 (2006) 389–395.
[28] N.H. Martin, R.M. Floyd, H.L. Woodcock, S. Huffman, C.-K. Lee, Computation of through-space NMR shielding effects in aromatic ring Pi-stacked complexes, J. Mol. Graphics Modell. 26 (2008) 1125–1130.
[29] N.H. Martin, B.W. Caldwell, K.P. Carlson, M.R. Teague, Ab initio calculation of through-space magnetic shielding of linear polycyclic aromatic hydrocarbons (acenes): extent of aromaticity, J. Mol. Graphics Modell. 27 (2009) 689–692.
[30] Titan, Version 1.0.1, Wavefunction Inc., Schrödinger Inc., 1999.
[31] W.J. Hehre, L. Radom, P.V.R. Schleyer, J.A. Pople, Ab Initio Molecular Orbital Theory, Wiley, New York, 1986.
[32] N.H. Martin, D.M. Loveless, D.C. Wade, A comparison of the calculated NMR shielding probes, J. Mol. Graphics Modell. 23 (2004) 285–290.
[33] M.J. Frisch, G.W. Trucks, H.B. Schlegel, G.E. Scuseria, M.A. Robb, J.R. Cheeseman, J.A. Montgomery Jr., T. Vreven, K.N. Kudin, J.C. Burant, J.M. Millam, S.S. Iyengar, J. Tomasi, V. Barone, B. Mennucci, M. Cossi, G. Scalmani, N. Rega, G.A. Petersson, H. Nakatsuji, M. Hada, M. Ehara, K. Toyota, R. Fukuda, J. Hasegawa, M. Ishida, T. Nakajima, Y. Honda, O. Kitao, H. Nakai, M. Klene, X. Li, J.E. Knox, H.P. Hratchian, J.B. Cross, C. Adamo, J. Jaramillo, R. Gomperts, R.E. Stratmann, O. Yazyev, A.J. Austin, R. Cammi, C. Pomelli, J.W. Ochterski, P.Y. Ayala, K. Morokuma, G.A. Voth, P. Salvador, J.J. Dannenberg, V.G. Zakrzewski, S. Dapprich, A.D. Daniels, M.C. Strain, O. Farkas, D.K. Malick, A.D. Rabuck, K. Raghavachari, J.B. Foresman, J.V. Ortiz, Q. Cui, A.G. Baboul, S. Clifford, J. Cioslowski, B.B. Stefanov, G. Liu, A. Liashenko, P. Piskorz, I. Komaromi, R.L. Martin, D.J. Fox, T. Keith, M.A. Al-Laham, C.Y. Peng, A. Nanayakkara, M. Challacombe, P.M.W. Gill, B. Johnson, W. Chen, M.W. Wong, C. Gonzalez, J.A. Pople, Gaussian 03, Revision B.01, Gaussian Inc., Pittsburgh, PA, 2003.
[34] S.F. Boys, F. Bernardi, The calculations of small molecular interaction by the difference of separate total energies. Some procedures with reduced error, Mol. Phys. 19 (1970) 553–566.
[35] TableCurve3D, Version 3.00A, AISN Software, San Rafael, CA, 1997.
[36] R. Chauvin, Explicit periodic trend of van der Waals radii, J. Phys. Chem. 96 (1992) 9194–9197.
[37] P.V.R. Schleyer, Private communication.
[38] N.H. Martin, J.D. Brown, K.H. Nance, H.F. Schaefer III, P.V.R. Schleyer, Z.-X. Wang, H.L. Woodcock, Analysis of the origin of through-space NMR (de)shielding by selected organic functional groups, Org. Lett. 3 (24) (2001) 3823–3826.